Seismic performance analysis of soft steel damper with single circular hole

Jinfeng Hao, Hao Liu*, Fawei Diao

College of Civil and Architecture Engineering, Northeast Petroleum University, Daqing, Heilongjiang, 163318, China

*Corresponding author's E-mail:3213316862@qq.com

Abstract. In order to investigate the effect of opening radius and different ways to change the cross-sectional area on the energy dissipation capacity of a single-circle hole mild steel damper, this paper changes the hole diameter by increasing the inner and outer diameters, keeping the radius difference unchanged, and expands the cross-sectional area of the damper by increasing the thickness, enlarging the outer diameter, and decreasing the inner diameter, and a total of 3 groups and 12 models were established to analyze the hysteresis curve, skeleton curve, energy dissipation-displacement curve, stress distribution and related simulation results of the dampers to evaluate their energy dissipation capacity through the reciprocating displacement loading mode. The study shows that the energy dissipation performance of the damper gets worse as the inner diameters and outer diameters increase more, and that decreasing the inner diameter improves the energy dissipation capacity more than increasing the outer diameter over increasing the thickness.

Keywords: disaster preparedness and mitigation, structural seismic defenses, mild steel damper.

1 Introduction

Since China is a country with frequent earthquakes. So the implementation of prefabricated structural buildings in China requires to be well protected against earthquakes. Metal dampers have been widely used to improve the seismic performance of building structures, and the installation of dampers at the beam-column nodes of prefabricated structures can effectively improve the seismic performance of the structure[1-2]. Single round hole soft steel damper has good hysteresis performance when subjected to shear and tensile compression. In previous studies, the energy is dissipated by the shear properties of the dampers, which are mostly set between the upper and lower beams of the frame structure. This setup method is not aesthetically pleasing, occupies space and wastes material. In order to solve these problems, we can rely on the tensile and compressive properties of the dampers to dissipate energy, and the dampers can be connected horizontally to the beam-column nodes of the assembled structure, which saves space and is easy to be replaced after damage. So we have done the following research.

A. M. Zende et al. (eds.), *Proceedings of the 2024 3rd International Conference on Structural Seismic Resistance, Monitoring and Detection (SSRMD 2024)*, Atlantis Highlights in Engineering 27,
https://doi.org/10.2991/978-94-6463-404-4_16

By changing the hole diameter by increasing the inner and outer diameters, keeping the radius difference unchanged; and changs the cross-sectional area of the energy dissipation section of the single-circular hole mild steel damper, their effects on the energy dissipation performance of the damper are studied. The aim is to provide a reference basis for the design direction to enhance the seismic capacity of dampers, and at the same time, promote the seismic development of beam-column nodes of assembled structures[3-4].

2 Moulding the damper

2.1 Design of damper dimensions

This paper changes the hole diameter by increasing the inner and outer diameters. Keeping the radius difference unchanged, and expands the cross-sectional area of the damper by increasing the thickness, enlarging the outer diameter, and decreasing the inner diameter. A total of three groups of 12 models are set up to study the effect of the aperture diameter of the circular hole opening and the different ways of changing the cross-sectional area on the energy dissipation capacity. The materials of the dampers are selected Q235 steel. The forms are shown in Figure 1. Figure a, b and c corresponds to D1, D2 and D3. The dimensions are shown in Table 1.

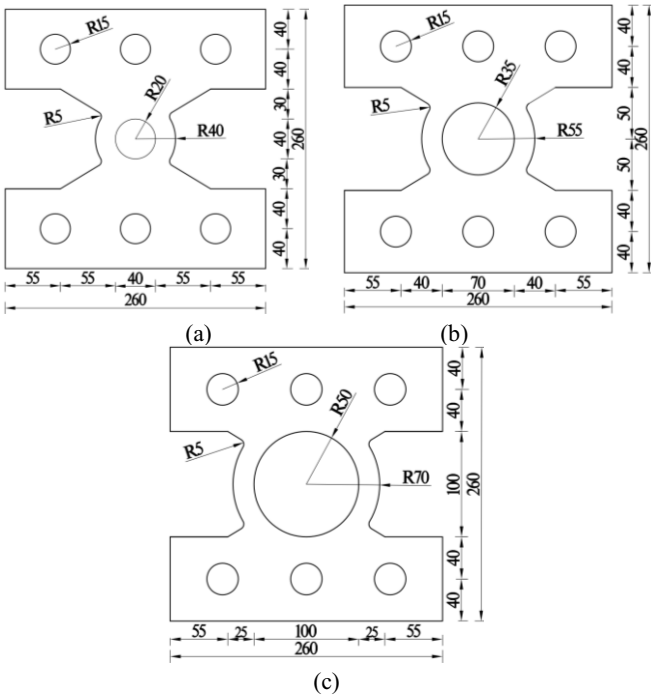

Fig. 1. Three types of single circular hole steel dampers.

Table 1. Size parameter table of damper specimens.

Damper	name	Overall size/mm	Connection section size/mm	t/mm	r_i/mm	r_e/mm	S/mm^2
D1	D1-Y	260×260	260×80	20	20	40	400
	D1-H	260×260	260×80	25	20	40	500
	D1-W	260×260	260×80	20	20	45	500
	D1-N	260×260	260×80	20	15	40	500
D2	D2-Y	260×260	260×80	20	35	55	400
	D2-H	260×260	260×80	25	35	55	500
	D2-W	260×260	260×80	20	35	60	500
	D2-N	260×260	260×80	20	30	55	500
D3	D3-Y	260×260	260×80	20	50	70	400
	D3-H	260×260	260×80	25	50	70	500
	D3-W	260×260	260×80	20	50	75	500
	D3-N	260×260	260×80	20	45	70	500

[a] t: Thicknesses.

[b] r_i: Inner diameter.

[c] r_e: Outer diameter.

[d] S: The cross-sectional area.

2.2 Steel Texture Relationships

The steel constitutive relationship adopts the bifold model, the stress-strain relationship is shown in Figure 2. The elastic modulus W after yielding is E_s=0.01E_0. The yield strength f_y of steel is taken as 235 MPa. The elastic modulus E_s is 2.06×105 MPa, and the Poisson's ratio is taken as 0.3. where σ_y is the yield strength of the steel; σ_u is the ultimate strength of the steel; σ_y is the yield strain corresponding to the yield strength σ_y of the steel; ε_u is the peak strain corresponding to the ultimate strength of steel σ_u; E_0 is the initial modulus of elasticity of steel bar; E_s is the modulus of elasticity of steel bar after yielding.

2.3 Cell selection and meshing

All mild steel damper specimens in the finite element model were modeled using an eight-node three-dimensional solid cell (C3D8R). The energy consuming regions were modeled with 2 mm mesh size and the other regions with 5 mm mesh size.

2.4 Interactions, loading regimes and analytical steps

The RP1 point is created at the upper end of the damper at the bolt hole, which is coupled to the surface of the bolt hole. At the same time, the node set is created at the RP1 point and named SET1, which serves as the node set for the subsequent result extraction. Set a completely fixed constraint at the lower end of the damper, apply vertical reciprocating displacement at point RP1 with displacement amplitudes of 0.25, 0.5,

0.75, 1, 1.5, 2, 2.5, 3, 3.5, 4, 4.5 and 5 (unit mm), as shown in Figure 3. A total of two analysis steps are set up. The lower end of the damper is completely fixed in the initial analysis step1. In step1, reciprocal displacement is applied to the damper at point RP1. And the field variable output and course output are set.

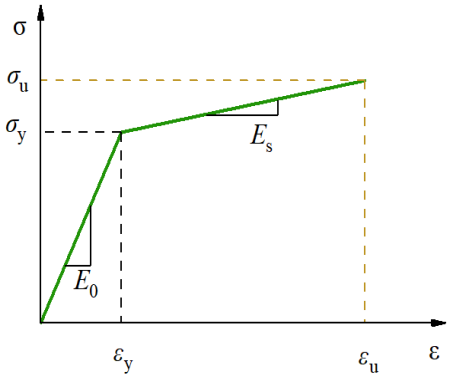

Fig. 2. Stress-strain curves of steel.

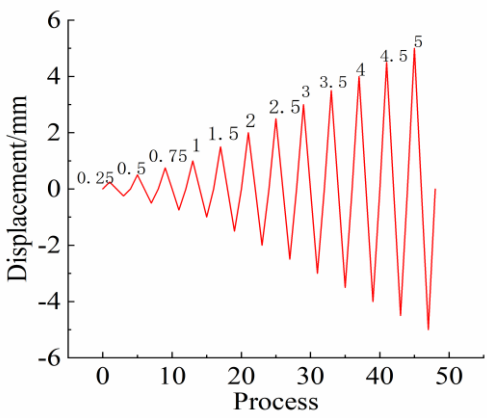

Fig. 3. Displacement loading curve.

3 Model validation

The damper used in the validation test is shown in reference [5]. For the above test, the test specimen was modeled according to ABAQUS as in Figure 4a. The skeleton curve results of the test and finite element analysis were compared as in Figure 4b, and the two skeleton curves basically coincided. The simulated specimen is first damaged at the end of the outer plate limb, and the damage morphology is shown in Figure 4c, which is consistent with the test damage morphology in Figure 4d. The yield displacement of the test specimen is 1.25mm, yield load is 10.04kN, and initial stiffness is 12.69kN/mm, while the yield displacement of the simulated specimen is 1.32mm, yield

load is 10.98kN, and initial stiffness is 12.73kN/mm with a difference of 5.6%, 9.4% and 0.3% respectively. The accuracy of ABAQUS simulation is proved.

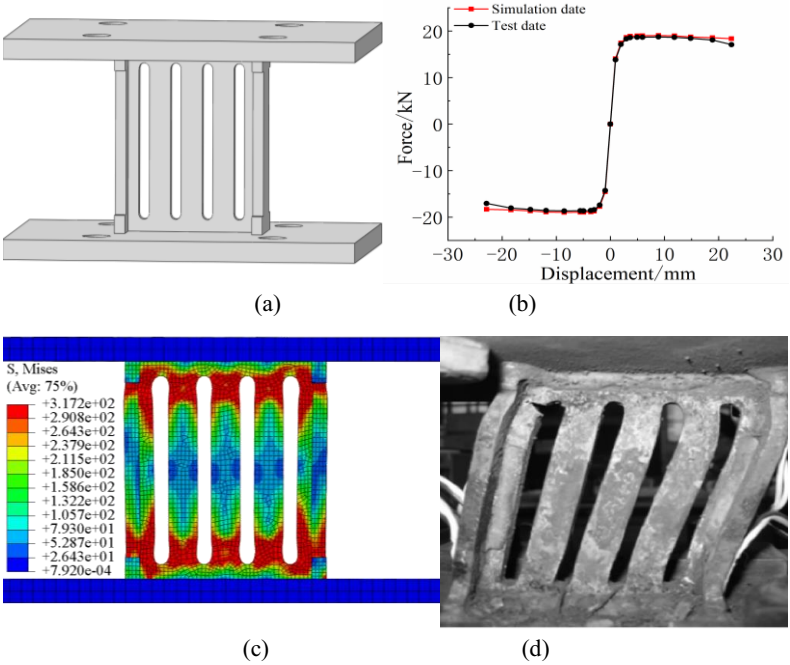

Fig. 4. Validation model and numerical simulation comparison chart.

4 Analysis of the effect of damper opening aperture and cross-sectional area

4.1 Analysis of hysteresis curves and simulation results

The simulation results of each specimen are shown in Table 2, and the hysteresis curve of each specimen is shown in Figure 5.

From Figure 5a, it can be seen that the hysteresis curves are full although the damper opening apertures are different, indicating that the specimens have good plasticity [6]. The hysteresis loop area becomes smaller as the damper opening radius increases. The hysteresis curve of the specimen is fuller in compression than in tension. From Table 2. In tension, the yield displacements of specimens D1-Y, D2-Y and D3-Y are 0.67 mm, 0.80 mm and 0.88 mm respectively. In compression the yield displacements are 0.61 mm, 0.67 mm and 0.73 mm respectively. In the tensile end, with the increase of radius, the yield displacements increase by 19.4% and 31.34% respectively. In the end of compression, the yield displacement increased by 9.84% and 19.67% respectively; the yield displacements of specimens D1-Y, D2-Y and D3-Y in tension decreased by 8.96%, 16.25% and 17.05% respectively, compared with those in compression. The

yield displacements at the compression end of the specimens are significantly smaller than those at the tension end.

For the damper with the same aperture diameter, after changing the cross-sectional area in three ways, it can be seen from Figure 5b, c and d that the hysteresis loop area increases after the cross-sectional area of the three groups of dampers D1, D2 and D3 increases, the trend of the change is similar. The cross-sectional area is increased by decreasing the inner diameter, which makes the energy dissipation capacity of the damper increase the most. By increasing the thickness, which makes the energy dissipation capacity increase the smallest. Taking the damper D3 in tension as an example, from Table 2 that the yield displacements of specimen D3-H, D3-W and D3-N formed after changing the cross-section of specimen D3-Y changed from 0.88 mm to 0.90 mm, 0.89 mm and 0.86 mm, the yield displacements of specimen D3-H and specimen D3-W increased by 2.27% and 1.14% respectively; the yield displacements of specimen D3-N decreased by 2.27% and 1.14%; the yield displacements of specimen D3-W decreased by 2.27% and 1.14%; the yield displacements of D3-N decreased by 1.14%. The yield displacement D3-N decreased by 2.27%.

Table 2. The results of the specimen simulation calculation.

Stress state	Damper	Name	P*y* /kN	Δ*y*/mm	P_{max} / kN	Δ*u*/mm	μ
Tension	D1	D1-Y	216.05	0.67	256.12	1.96	2.93
		D1-H	273.42	0.68	323.54	1.95	2.87
		D1-W	274.88	0.68	321.48	1.99	2.93
		D1-N	275.51	0.65	327.18	1.94	2.98
	D2	D2-Y	202.75	0.80	244.66	2.94	3.68
		D2-H	255.03	0.81	308.77	2.97	3.67
		D2-W	255.40	0.79	309.47	2.93	3.71
		D2-N	259.70	0.76	313.20	2.95	3.88
	D3	D3-Y	186.39	0.88	226.73	2.98	3.39
		D3-H	237.69	0.90	288.35	2.93	3.26
		D3-W	242.19	0.89	295	2.94	3.30
		D3-N	246.90	0.86	300.63	2.97	3.45
Pressure	D1	D1-Y	225.59	0.61	261.06	3.19	5.32
		D1-H	284.11	0.62	329.47	3.24	5.23
		D1-W	292.21	0.63	331.26	3.29	5.22
		D1-N	304.30	0.63	341.02	3.30	5.24
	D2	D2-Y	202.04	0.67	243.84	2.94	4.39
		D2-H	254.99	0.68	307.57	2.97	4.37
		D2-W	260.09	0.69	310.86	2.94	4.26
		D2-N	268.20	0.67	316.46	2.96	4.42
	D3	D3-Y	182.29	0.73	224.03	2.48	3.40
		D3-H	230.75	0.75	284.42	2.44	3.25
		D3-W	240.34	0.76	293.97	2.45	3.22
		D3-N	246.58	0.74	300	2.48	3.35

[a] *Py*: Yield load.

[b] Δ*y*: Yield displacement.

[c] P_{max}: peak load.

[d] Δ*u*: Peak displacement.

[e] μ: Ductility factor.

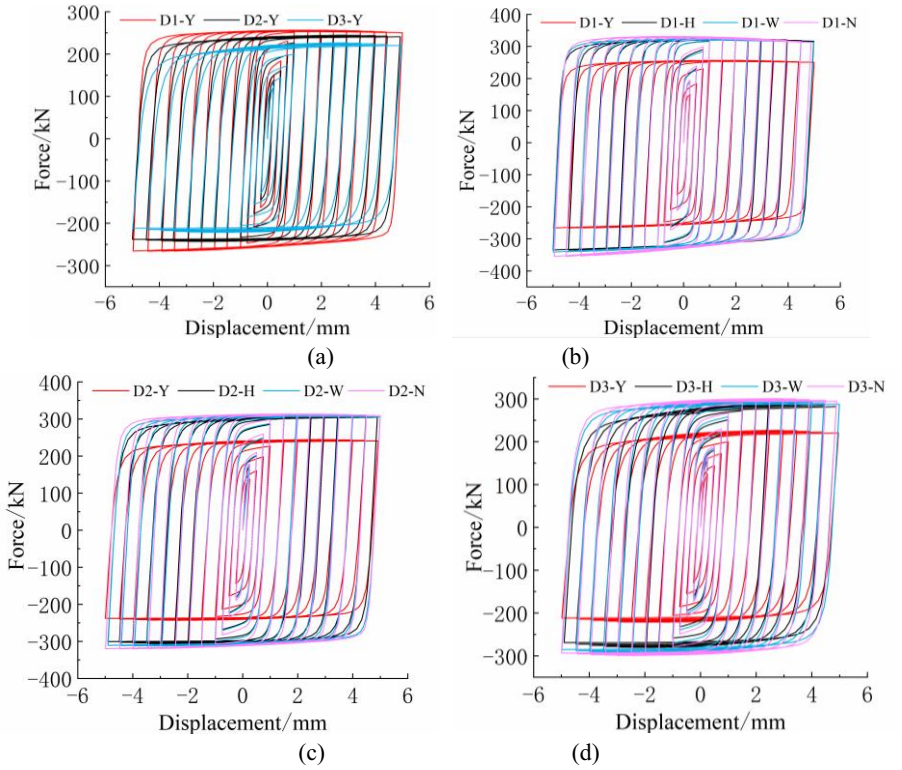

Fig. 5. Hysteresis curves of three groups of damper specimens.

4.2 Analysis of Skeleton curve

Figure 6 shows the skeleton curves of the dampers. From Figure 6a, the individual specimen skeleton curves exhibit bilinear characteristics and distinct yield points.At the beginning of loading, small displacement can make the damper yield rapidly, and with the increase of displacement, the load remains constant after a small increase and enters the plastic deformation stage, and the energy dissipation performance of the damper is good and stable.

The inner and outer diameters of D1-Y, D2-Y and D3-Y were increased, when the radius difference was kept unchanged. From Figure 7b and Table 2, it can be obtained that the yield load of the dampers decreased. In tension, the yield load decreased from 216.05 kN to 202.75 kN and 186.39 kN; reduced by 6.16% and 13.73% respectively; and in compression, the yield load decreased from 225.59 kN to 202.04kN and 182.29kN; reduced by 10.44% and 19.19% respectively.

From Figure 6c and Table 2, it can be seen that the yield load also increases after the increase in the cross-sectional area of the same damper, which ranges from 25.79% to 35.27%. Taking the D2 as an example, the yield loads of specimens D2-Y, D2-H, D2-W, and D2-N are 202.75 kN, 255.03 kN, 255.40 kN and 259.70 kN respectively. specimens D2-H, D2-W and D2-N have an increase of 25.79% in yield loads respectively,

with respect to D2-Y, loads increased by 25.79%, 25.97% and 28.09% respectively. The specimen D2-N formed after reducing the inner diameter has the better energy dissipation.

From Figure 6d, it can be seen that D1-N has the maximum yield load and D3-N has the minimum yield load. The ductility coefficient of specimen D1-N is the largest, specimen D2-N is the second largest and specimen D3-N is the smallest. The energy dissipation of specimen D1-N is the best when it is under pressure.

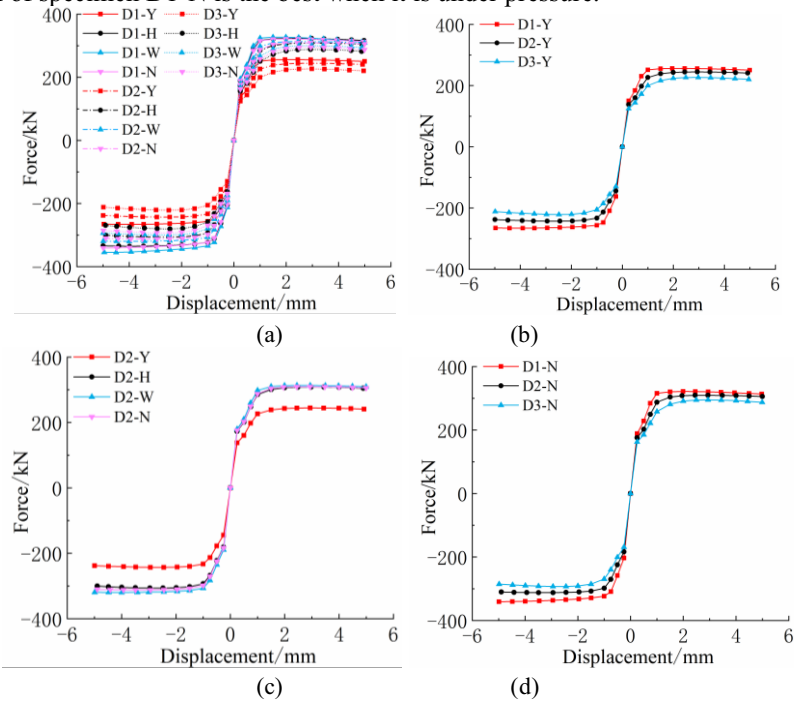

Fig. 6. Skeleton curve of the damper specimen.

4.3 Analysis of stress map

The stress clouds of D1-Y, D2-Y and D3-Y are shown in Figure 7. Under the action of etensile(or pressure) and bending moment generated by eccentricity, there is a difference between the stress state of the inner and outer sides of the circle, which is manifested as the stress of the inner side is larger than that of the outer side, but as the diameter of the circular hole aperture increases, the effect of eccentricity decreases, and the difference gradually decreases. The stress distribution of the test damper (see Figure 4c) is mainly concentrated in the end of the plate limb. The energy-consuming section is not fully involved in energy dissipation; while the stress distribution of the single-circular-hole damper is concentrated in the energy-consuming section (see Figure 7), and the stress distribution of each damper specimen is uniform. The part of the participating energy-consuming part is mainly concentrated in the weak section at the hole.

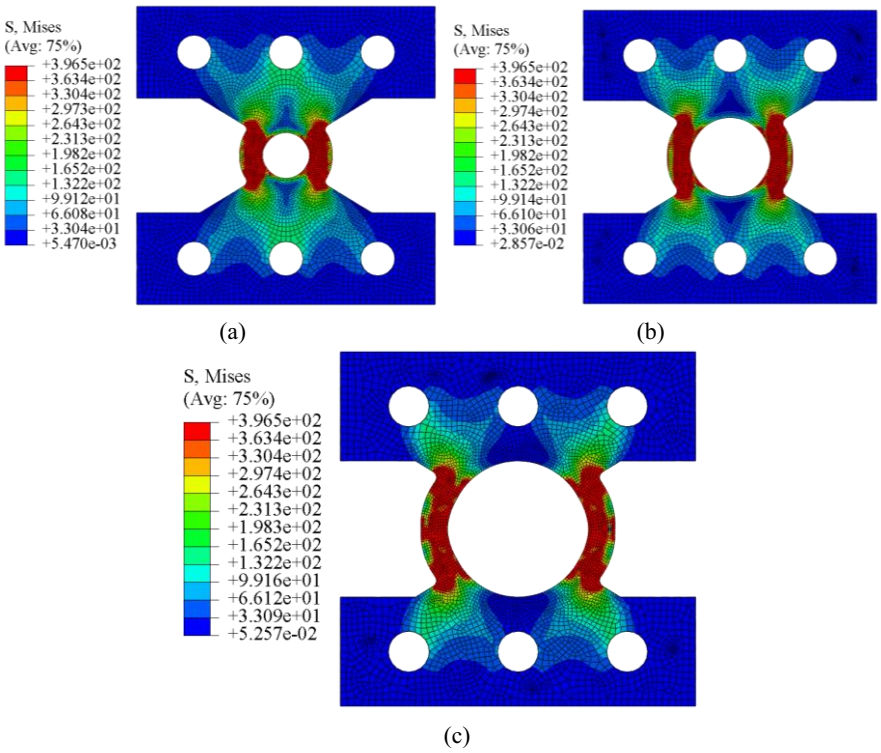

Fig. 7. Stress contour of a partial damper specimen.

5 Conclusions

Taking the opening aperture of single round hole mild steel damper and different ways to increase the cross-sectional area as the examination factors, finite element analysis of 3 groups of 12 damper specimens designed were carried out. The following conclusions were drawn:

(1) When the opening radius of the damper is small, due to the large influence of eccentricity, resulting in the existence of differentiated stress state between the inner and outer sides of the specimen. With the increase of the opening radius, the eccentricity gradually decreases, and the differentiation between the inner and outer stresses is gradually weakened. The energy dissipation performance also becomes more stable.

(2) With the increase of the cross-sectional area of the damper, the energy dissipation performance of the damper continues to improve. The better the seismic performance; in the case of the same cross-sectional area, the way of reducing the inner diameter has better energy dissipation effect and better seismic performance.

(3) The stress distribution of the damper is uniform, and the energy dissipation performance is stable when an earthquake comes. Important for the development of seismic resistance of nodes in assembled structures.

References

1. Chen Y, Chen C and Jiang H (2019) Study of an innovative graded yield metal damper. Journal of Constructional Steel Research, 160: 240-254. 10.1016/j.jcsr.2019.05.028.
2. Guo W, Li S and Zhai Z (2022) Seismic performance of a new S-shaped mild steel damper with varied yielding cross-sections. Journal of Building Engineering, 45: 103508. 10.1016/j.jobe.2021.103508.
3. Teruna D R, Majid T A and Budiono B (2015) Experimental study of hysteretic steeldamper for energy dissipation capacity. Advances in Civil Engineering, 2015: 1-12. https: //doi. org/10.1155/2015/631726.
4. Jaisee S, Yue F and Ooi Y H (2021) A state-of-the-art review on passive friction dampers and their applications. Engineering Structures, 2021, 235: 112022. 10.1016/j.engstruct. 2021.112022.
5. LU X L, Zhu Q Y (2019) Shaking table test of earthquake-damaged recycled aggregate concrete frame retrofitted with steel dampers.47(07):0914~0924. 10.11908/j.issn.0253-374x. 2019.07.003.
6. Gao H G, Zhang L X and Shi X X (2020) Research on seismic performance of Z-supported graded yield damper. Civil Engineering Journal, 53(S2): 94-100. 10. 15951/ j. tmgcxb. 2020. s2.015.